A mechanism of covalent substrate binding in the x-ray structure of subunit K of the *Escherichia coli* dihydroxyacetone kinase

Christian Siebold*†, Luis Fernando García-Alles*, Bernhard Erni*‡, and Ulrich Baumann*‡

*Departement für Chemie und Biochemie, Universität Bern, Freiestrasse 3, CH-3012 Bern, Switzerland

Communicated by Saul Roseman, The Johns Hopkins University, Baltimore, MD, May 9, 2003 (received for review September 2, 2002)

Dihydroxyacetone (Dha) kinases are homologous proteins that use different phosphoryl donors, a multiphosphoryl protein of the phospho*enol*pyruvate-dependent carbohydrate:phosphotransferase system in bacteria, ATP in animals, plants, and some bacteria. The Dha kinase of *Escherichia coli* consists of three subunits, DhaK and DhaL, which are colinear to the ATP-dependent Dha kinases of eukaryotes, and the multiphosphoryl protein DhaM. Here we show the crystal structure of the DhaK subunit in complex with Dha at 1.75 Å resolution. DhaK is a homodimer with a fold consisting of two six-stranded mixed β-sheets surrounded by nine α-helices and a β-ribbon covering the exposed edge strand of one sheet. The core of the N-terminal domain has an α/β fold common to subunits of carbohydrate transporters and transcription regulators of the phospho*enol*pyruvate-dependent carbohydrate:phosphotransferase system. The core of the C-terminal domain has a fold similar to the C-terminal domain of the cell-division protein FtsZ. A molecule of Dha is covalently bound in hemiaminal linkage to the Nε2 of His-230. The hemiaminal does not participate in covalent catalysis but is the chemical basis for discrimination between short-chain carbonyl compounds and polyols. Paralogs of Dha kinases occur in association with transcription regulators of the TetR/QacR and the SorC families, pointing to their biological role as sensors in signaling.

glycerone | hemiaminal | phospho*enol*pyruvate | phosphotransferase | transcription regulation

Dihydroxyacetone (Dha) kinases convert free Dha into the glycolytic intermediate Dha phosphate (DhaP). In methylotrophic yeast, Dha is the primary product of methanol assimilation (1). In bacteria, Dha is formed by oxidation of glycerol or aldol cleavage of fructose-6-phosphate (2, 3). In animal cells, Dha is a gluconeogenic precursor (4–6). The Dha kinase of *Escherichia coli* was discovered in the proteome as two spots, which were up-regulated in the *ptsI* mutant, lacking enzyme I of the phospho*enol*pyruvate(PEP)-dependent carbohydrate:phosphotransferase system (PTS) (7) and displayed strong amino acid sequence similarities to the N- and C-terminal domains of the ATP-dependent Dha kinase of *Citrobacter freundii* (7, 8). The two subunits, termed DhaK and DhaL (SWISS-PROT entries P76015 and P76014), are encoded in an operon together with a third protein, DhaM (SWISS-PROT entry P37349). DhaM is a multiphosphoryl protein of the PTS with sequence similarity to the IIA domain of the mannose transporter (PDB ID code 1PDO; ref. 9), the phosphoryl carrier protein HPr (PDB ID code 1PTF; ref. 10) and the N-terminal domain of enzyme I (PDB ID code 1ZYM; ref. 11). DhaM is phosphorylated by PEP through enzyme I and the phosphoryl carrier protein HPr and serves as the phosphoryl donor instead of ATP (12):

$$\text{PEP} \rightarrow \text{EI} \rightarrow \text{HPr} \rightarrow \text{DhaM} \xrightarrow{\text{DhaK/DhaL}} \text{Dha}$$

No similarity with known protein folds could be predicted for DhaK and DhaL. DhaK, DhaL, and DhaM were overexpressed and purified (12). Whereas DhaL precipitates already at low protein concentration, DhaK is soluble. Here we describe the x-ray structure of DhaK with Dha covalently bound to a histidine in the active site.

Materials and Methods

Protein Purification and Activity Assay. *E. coli* DhaK was overproduced in *E. coli* WA2127ΔHIC(*ptsI*) as described (12) and purified by ion exchange chromatography over DEAE cellulose (C545, Fluka) and ResourceQ (Amersham Pharmacia) and gel filtration over Superdex 200 (Amersham Pharmacia). DhaK was concentrated to 30 mg·ml^{-1} in 5 mM Hepes, pH 7.5/2 mM DTT. The apoform of DhaK was generated between DEAE and ResourceQ chromatography by incubation of the DhaK–Dha complex with PEP and catalytic amounts of the PTS proteins (enzyme I, HPr) DhaM and DhaL. DhaK activity was measured in a coupled assay by reduction of DhaP with glycerol-3-phosphate dehydrogenase. The disappearance of NADH was monitored continuously in a Spectramax 250 plate reader (Molecular Devices) at 30°C (12).

Crystallization and Data Collection. The DhaK–Dha complex and the apoprotein were crystallized from 80 mM sodium acetate, pH 5.0/160 mM $(NH_4)_2SO_4$/17% (wt/vol) polyethylene glycol (PEG) 4000/15% (wt/vol) 2-methyl-2,4-pentanediol (MPD) using hanging drop vapor diffusion. The crystals had the symmetry of the space group $P2_12_12$ (a = 96.5 Å, b = 97.4 Å, c = 86.0 Å, $\alpha = \beta = \gamma = 90°$) and they diffracted to 1.75 Å resolution after flash-freezing at 105° K in the native mother liquor. Native and derivative diffraction data were collected on a RAXIS-IV imaging plate detector mounted on a Rigaku RU300 generator equipped with Yale mirrors (Molecular Structure, The Woodlands, TX). All data were processed by using the HKL program package (13).

Structure Solution and Refinement. The DhaK structure was determined by the multiple isomorphous replacement (MIR) method. Heavy-atom sites were located with SHELX (14). Phases were calculated by using SHARP (15) and improved by solvent flattening by using the program SOLOMON (16). An initial protein model was built into the electron density by using the programs ARP/WARP (17) and O (18). Noncrystallographic symmetry restraints were used to refine the model at 1.75 Å

Abbreviations: Dha, dihydroxyacetone; DhaP, Dha phosphate; DhaK, DhaL, and DhaM, subunits of the *Escherichia coli* Dha kinase; PEP, phospho*enol*pyruvate; PTS, PEP-dependent carbohydrate:phosphotransferase system; Trp, tryptophan.

Data deposition: The atomic coordinates and structure factors have been deposited in the Protein Data Bank, www.rcsb.org [PDB ID codes 1OI2 (for subunit K of the *E. coli* dihydroxyacetone kinase bound to dihydroxyacetone) and 1OI3 (for subunit K of the *E. coli* dihydroxyacetone kinase in its apo-form)].

†Present address: Division of Structural Biology and Oxford Protein Production Facility, Roosevelt Drive, Oxford OX3 7BN, United Kingdom.

‡To whom correspondence may be addressed: E-mail: erni@ibc.unibe.ch or ulrich.baumann@ibc.unibe.ch.

www.pnas.org/cgi/doi/10.1073/pnas.0932787100

Table 1. Crystallographic data, structure solution, and refinement statistics

	DhaK–Dha complex	Ta_6Br_{14}	$KAu(CN)_2$	PIP*	Apo–DhaK
Data collection					
Resolution, Å†	1.75 (1.78–1.75)	2.45 (2.52–2.45)	2.45 (2.55–2.45)	2.45 (2.55–2.45)	2.0 (2.04–2.00)
Unique reflections	78,957	29,777	27,533	30,483	51,496
Redundancy	3.7	3.1	2.3	2.4	2.9
Completeness, %†	95.7 (97.5)	99.8 (99.3)	94.4 (90.4)	96.2 (93.6)	93.1 (60.6)
I/σ (I)	19.4	21.3	23.4	21.6	23.7
R_{merge}, %†‡	4.6 (17.2)	4.6 (7.4)	3.5 (6.4)	4.3 (7.9)	4.6 (10.0)
Structure solution					
Resolution range, Å		25.0–4.5	25.0–2.5	25.0–2.5	
Heavy-atom sites		6	5	4	
Phasing power (acentric/centric)		3.0/2.7	2.0/1.5	1.3/1.3	
R_{Cullis} (acentric/centric)		58.1/55.4	67.1/69.1	81.7/79.6	
Refinement statistics					
Resolution range, Å	25.00–1.75				25.00–2.00
R_{factor}§/R_{free}¶ %	17.15/20.1				18.9/23.8
rmsd bond lengths, Å	0.012				0.018
rmsd bond angles, °	1.618				1.780
No. of reflections	76,798				50,052
No. of protein atoms	5,026				5,026
No. of water molecules	508				485

rmsd, root-mean-square deviation from ideal geometry.

*PIP, Di-μ-iodobis(ethylenediamine) diplatinum (II)-nitrate.

†Numbers in parentheses refer to the indicated highest resolution shell.

‡$R_{merge} = \Sigma_{hkl}\Sigma_i|(hkl; i) - \langle(hkl)\rangle|/\Sigma_{hkl}\Sigma_i(hkl; i)$, where $I(hkl; i)$ is the intensity of an individual measurement and $\langle I(hkl)\rangle$ is the average intensity from multiple observations.

§$R_{factor} = \Sigma_{hkl}||F_{obs}| - k|F_{calc}||/\Sigma_{hkl}|F_{obs}|$.

¶R_{free} = the R factor against 5% of the data removed prior to refinement.

resolution by using the program REFMAC (19). Details of the crystallographic analysis are shown in Table 1.

Results

Structure Determination and Overall Architecture. The structure of DhaK was solved by MIR at 2.5 Å resolution. Refinement against 1.75-Å data resulted in an R factor of 17.1% and an R_{free} of 20.1%, with excellent stereochemistry (Table 1). The asymmetric unit contains one physiological dimer (Fig. 1*A*). Residues 20–368 of the DhaK monomer are well ordered, with the exception of residues 205–217. The monomer can be divided into two domains, with each composed of a six-stranded β-sheet, which are covered by α-helices (Fig. 2*A*).

The core of the N-terminal domain (residues 55–195) possesses a similar fold as the IIA domain of the mannose transporter (PDB ID code 1PDO; ref. 9). It consists of a central four-stranded parallel β-sheet surrounded by 5 helices (Fig. 2, blue boxed area). Helix 4 and 5 form a hairpin, which is characteristic of the IIA fold. Overlay of the DhaK core with the IIA domain using the DALI server (20) yields a Z score of 9.3 and an rms deviation of 2.5 Å for 106 C^α atoms (Fig. 3, red and blue backbone traces). The IIA core of DhaK is extended on the N-terminal side by two antiparallel strands (residues 33–54) and the dimerization helix 1 (residues 20–32). On the C-terminal side it is connected to the next domain. This second domain also consists of a six-stranded mixed β-sheet (Fig. 2). It is covered by two helices on the solvent-exposed side and packed against the first helix of the helix hairpin (residues 161–175) on the other side. The C-terminal 15 residues of the polypeptide chain fold back onto the N-terminal domain. The fold assumed by the leftmost four β-strands and the two solvent-exposed helices (Fig. 2*A*, green boxed area) also occurs in the C-terminal domain (residues 249–339) of the bacterial cell-division protein FtsZ of *M. jannaschii* (Fig. 3, green backbone traces, PDB ID code 1FSZ; ref. 21) with a Z score of 5.8 and an rms deviation of 2.3 Å for 72 C^α atoms. Inserted into this common fold is the active site

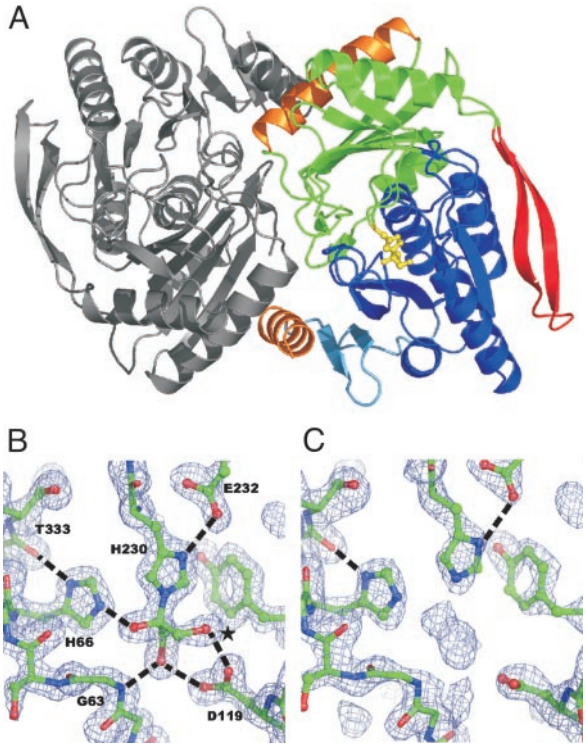

Fig. 1. Structure of the DhaK–Dha complex. (*A*) Ribbon diagram of the DhaK dimer. The subunits are gray, the N-terminal domain is blue, the C-terminal domain is green, the β-ribbon is red, and the contact helices are orange. The atoms of His-230 with Dha in a hemiaminal linkage are shown as a yellow stick model. (*B* and *C*) Experimental 2 Fo-Fc electron densities of the active site complexed with Dha and empty at 1.75-Å resolution contoured at 1.5 σ. Hydrogen bonds are indicated as black dotted lines. Only the *pro-R* OH (*) is surface exposed.

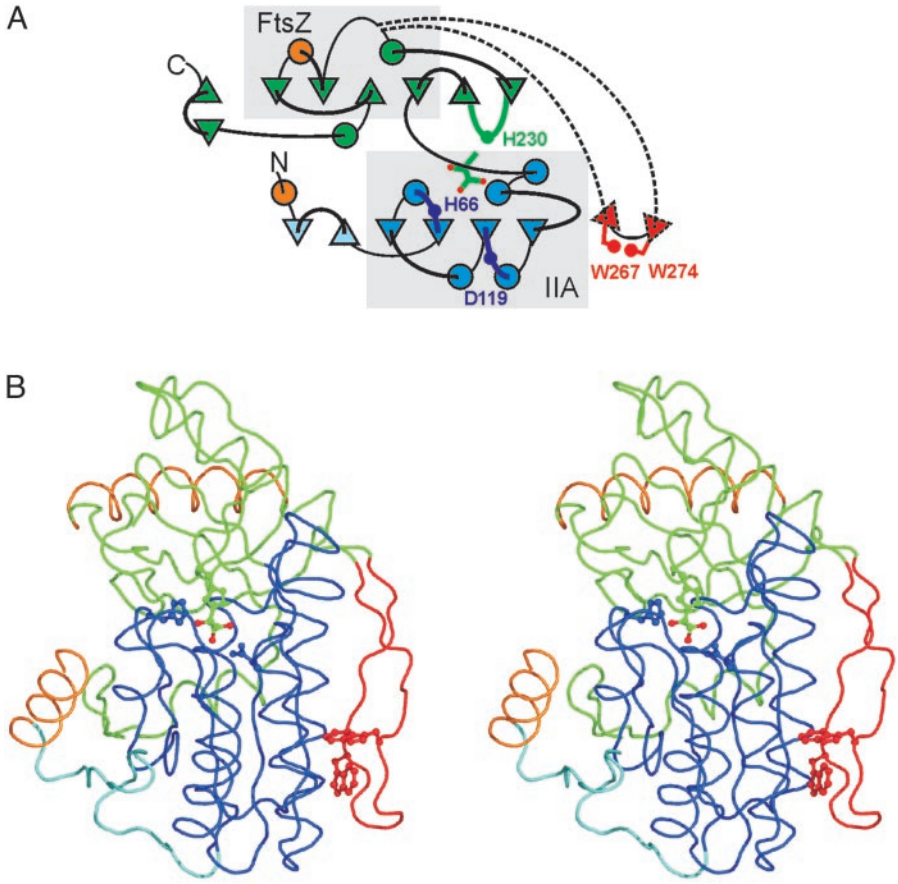

Fig. 2. Models of DhaK subunit colored by structural entities. (*A*) Folding diagram. β-strands depicted by a Δ are running downward. For clarity, the folding diagram of the upper sheet has been rotated +60° around an axis perpendicular to the lower sheet. (*B*) Stereoview of backbone related to Fig. 1*A* by a 50° rotation around the horizontal axis. The N-terminal domain is cyan and the IIA core is blue (boxed area), the C-terminal domain is green with the FtsZ core boxed, the β ribbon is red, and contact helices 1 and 8 are orange. The hemiaminal between His-230 and Dha and His-66 and Asp-119 are depicted in the green and blue ball-and-stick representation, and the Trp-267/Trp-274 zipper in the red ball-and-stick representation.

loop of DhaK consisting of two short antiparallel β-strands bearing the active site His-230. The DhaK dimer interface is formed by helices 1 and 8 (Fig. 2), which intersect at an angle of 70°. A total of 9.3% (2,390 Å^2) of the accessible surface is buried on dimer formation.

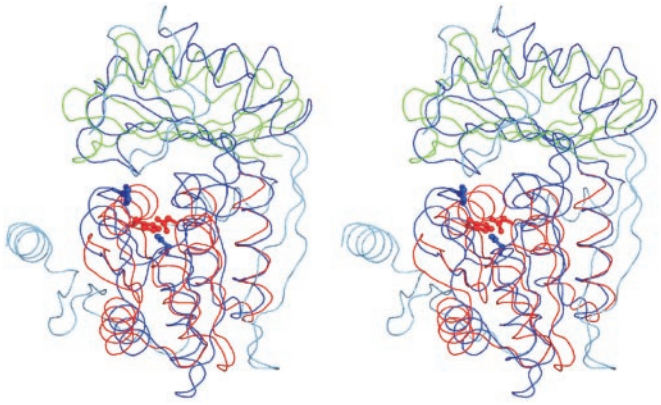

Fig. 3. Superposition of backbone traces of DhaK (blue), IIA^{Man} (red), and the C-terminal domain of FtsZ (green, residues 249–339). The conserved histidine and aspartic acid residues at the topological switch points of the fold are indicated in ball-and-stick representation. Superimposable regions of DhaK are dark blue; nonalignable regions are light blue.

The Twisted Two-Strand β-Ribbon. A prominent feature on the outer surface of DhaK is a β-ribbon (Fig. 2, residues 255–284), which caps the edge of the N-terminal β-sheet (residues 137–142). It is inserted between the first helix and second β-strand of the FtsZ fold. The ribbon contains two conserved tryptophans (Trp-267 and Trp-274), which form a Trp zipper, a motif that is proposed to stabilize β-hairpins in their strongly twisted conformation (22, 23). A comparison of homologous Dha kinase sequences reveals that the β ribbon is present only in DhaK of Gram-negative bacteria, where it covers an edge strand, which is composed exclusively of hydrophobic residues. In the Dha kinases of Gram-positive bacteria and eukaryotes, the corresponding edge strand contains a glutamic acid residue. Charged residues and β-ribbons are devices that have been proposed to protect edge strands of regular β-sheets from aggregation with any other β-strands they encounter (23). The ribbon itself is constrained by the Trp zipper and thereby protected from aggregation into a larger β-sheet.

Dha-Binding Site. Unexpected electron density at His-230 in the C-terminal domain could unambiguously be assigned to a molecule of Dha bound as a hemiaminal to the Nε2 of the imidazole ring (Fig. 1*B*). The covalently bound substrate is further held in place by a network of hydrogen bonds to residues of the N-terminal domain. The geminal aminoalcohol group at C-2 of Dha forms a hydrogen bond with the Nε2 of His-66, and the OH groups at C1 and C3 are coordinated by the carboxyl group of

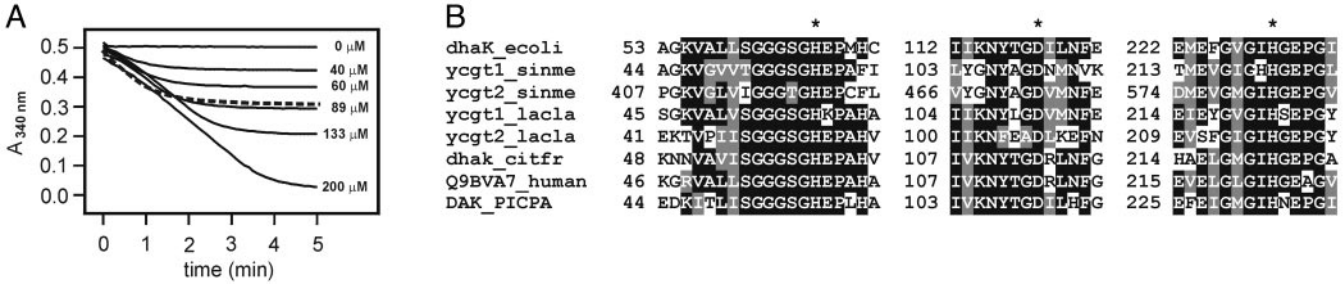

Fig. 4. Activity and amino acid sequence of the active site. (*A*) Liberation of DhaP from the DhaK–substrate complex. Highly purified DhaK (110 μM) was incubated with an excess of PEP and catalytic amounts of EI, HPr, DhaL, and DhaM. The release of DhaP (broken line) was monitored by its reduction with glycerol-3-phosphate dehydrogenase. DhaP at the indicated concentrations was reduced in parallel (solid lines). (*B*) Alignment of the active-site sequences of representative PEP-dependent and ATP-dependent DhaK orthologs and of two representative paralogs involved in transcription control. *, His-66, Asp-119, and His-230. DhaK of *E. coli* (SWISS-PROT entry P76015), YcgT1 of *Sinorhizobium meliloti* (SWISS-PROT entry Q92WN2; ref. 37), and *Lactococcus lactis* (Q9CIV8; ref. 38) are subunits of PEP-dependent Dha kinase. YcgT2 of *S. meliloti* (SWISS-PROT entry Q92WN4) and *L. lactis* (SWISS-PROT entry Q9CIW0) are domains and subunits of putative transcription regulators of the SorC and TetR/QacR families. DhaK and DAK are ATP-dependent Dha kinases of *C. freundii* (SWISS-PROT entry P45510), man, and the yeast *Pichia pastoris* (SWISS-PROT entry O74192).

Asp-119 and the main-chain amide hydrogen of Gly-63 (Fig. 1*B*). His-230 is at the turn of a loop suspended from the two rightmost β-strands of the C-terminal domain, its imidazole ring being fixed by a hydrogen bond between the Nδ1 and the side-chain carboxylate of Glu-232. His-66 and Asp-119 are at the topological switch point of the core fold common to DhaK and IIA^{Man} (Fig. 3). The imidazole ring of His-66 is held in place by a hydrogen bond between its Nδ1 atom and the main-chain carbonyl oxygen of Thr-333.

Dha is buried in a cavity. Only the *pro-R* OH group (Fig. 1*B*) is surface exposed and ready for a electrophilic attack by phospho-His-9 of DhaM (12). Dha binding must be tight because no substrate was added at any stage of the protein purification. By chance, Dha also was not removed *in vivo*, because DhaK was expressed in a *ptsIptsH* strain, where DhaM cannot be phosphorylated and Dha is consequently not phosphorylated either (12). In fact, $\approx$0.8 mol of DhaP per mol of DhaK are readily released *in vitro* on incubation of the complex with PEP and catalytic amounts of the phosphotransferase components enzyme I, HPr, DhaM and DhaL (Fig. 4A). This indicates that Dha is bound to the active and not to an allosteric site. Consistent with this conclusion is the observation that mutations of His-230 to alanine or lysine completely abolished kinase activity (results not shown).

DhaK was freed of Dha by incubation with DhaL and the PTS components, the apoprotein crystallized under the same condition as the DhaK–Dha complex, and the structure solved at 2.0 Å resolution (Table 1). The difference Fourier map with phases derived from the DhaK–Dha complex model revealed strong extra-negative density at the position of the covalently bound Dha molecule. But otherwise, removal of Dha did not detectably alter the conformation of the active site (Fig. 1*C*).

The Family of DhaK Paralogs. A BLASTP (24) search revealed genes for DhaK-like protein subunits and domains in >50 Gram-positive and Gram-negative bacteria as well as in many eukaryotes. PTS-dependent and ATP-dependent Dha kinases are discernible by phylogenetic clustering but no sequence motif emerged which could be considered to be critically relevant for phosphoryl donor recognition. A second operon for putative transcription regulators and DhaK-like proteins is often found immediately adjacent to the catalytic operon (Fig. 5). Assuming that proteins encoded in an operon are functionally related, it is likely that these DhaK-like proteins are paralogs with regulatory functions. The active site residues are also invariant in these paralogs (Fig. 4*B*). Fig. 5 shows relationships by fold and function of representative examples. A two-domain protein of *Sinorhizobium meliloti* consists of an N-terminal domain belonging to the SorC family of transcription regulators (25) and a DhaK-like C-terminal domain. A DhaK paralog of *Lactococcus lactis* is encoded in an operon together with YceG, a protein belonging to the TetR/QacR (26, 27) family of repressors. It remains to be elucidated how the DhaK paralogs are activated by ligand binding and whether the activated state is eventually terminated by phosphorylation of the ligand in a PTS-dependent reaction.

Discussion

The x-ray structure of the DhaK subunit of the *E. coli* Dha kinase reveals that Dha is bound by a hemiaminal linkage between the imidazole ring and the carbonyl group. Hemiaminals are generally unstable. Those with primary amines react further by elimination of water to give Schiff bases or enamines. Those with secondary amines can form enamines if an α-hydrogen is present but not a Schiff base. In the DhaK active site the hemiaminal is stabilized by a hydrogen bond between the geminal alcohol and the imidazole ring of His-66. We propose that this hemiaminal does not directly participate in chemical catalysis, in contrast to the hemithioacetal intermediate of glyceraldehyde-3-phosphate dehydrogenase or the Schiff base intermediate of an aldolase (28). The experiments in support of this conclusion are (L.F.G.-A., unpublished data): (*i*) Glyceraldehyde and erythrose are phos-

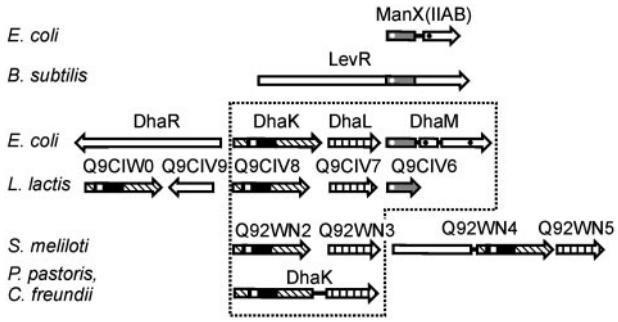

Fig. 5. Domain and subunit composition of representative Dha kinases and their associated transcription regulators. The catalytic Dha kinase subunits are framed (dotted line). Homologous subunits and domains are labeled as follows: DhaK-like (slanted lines) and DhaL-like (vertical lines). The IIA folds are gray and the core fold of DhaK is black. The invariant His are indicated by white dots (phosphorylation sites) and white squares (hydrogen bonding of Dha). Established and putative transcription regulators are indicated as open arrows. ManX is a subunit ($IIAB^{Man}$) of the mannose transporter. The horizontal alignment of the proteins reflects the organization of the respective operons. Functionally characterized proteins are indicated by their gene names, proteins for which a function is suggested are indicated by their SWISS-PROT entry number.

phorylated by the Dha kinase at the β-OH and the γ-OH, respectively, and not like Dha at the α-OH. Similarly, a tomato enzyme homologous to the Dha kinase phosphorylated 3,4-dihydroxy-2-butanone at OH-4, and not at OH-3 (29). (*ii*) Substrate and product are both covalently bound. Strong electron density at His-230 reappears after soaking crystals of substrate-free DhaK with DhaP. The equilibrium dissociation constants of DhaK are 8 μM for Dha and 1.6 mM for DhaP. At a physiological DhaP concentration of $\approx$50 μM (30) product inhibition of DhaK is minimal. (*iii*) No exchange of hydrogen against deuterium at C-1 of Dha could be detected when the Dha kinase reaction was performed in D_2O. This finding suggests that no enamine is formed that could increase the acidity of the α-OH. In conclusion, it appears improbable that the hemiaminal affects the reactivity of the α-OH. Such an effect is even less plausible for the β-OH and γ-OH of glyceraldehyde and erythrose, which are separated from the hemiaminal by one and two extra carbon–carbon bonds.

Covalent binding of substrates by bonds that do not participate in the catalyzed reaction is unusual, and to our knowledge, has not been observed before. What might be its function? We propose that formation of the hemiaminal is the chemical basis for efficient discrimination between short-chain ketoses and aldoses on one hand and the structurally similar polyalcohols on the other. The former are chemically reactive and potentially toxic, even at low concentrations (31, 32). The latter are compatible solutes, which accumulate to high concentrations as osmoprotectants, for instance in yeast (33). Removing a potentially noxious compound in the presence of a neutral or beneficial requires strong discrimination. In accord with this idea, glycerol in concentrations up to 20% (2.2 M) is neither a substrate nor an inhibitor of *E. coli* Dha kinase which, however, turns over the small amounts of contaminants present in commercial glycerol lots (unpublished data). On the other hand, glycerol kinases, which form no covalent intermediates and therefore may lack the specific discrimination between carbonyl compounds and polyols, do phosphorylate both glycerol and Dha (34, 35).

Dha kinases exist in two forms: ATP-dependent, and PEP-dependent. In eukaryotes that do not have a PTS, all Dha kinases are ATP-dependent. In bacteria most Dha kinases are PEP-dependent and only a few (for instance, *C. freundii*) are ATP-dependent. Strong amino acid sequence conservation suggests that all Dha kinases have a common ancestor, which, according to the results of phylogenetic clustering, might have been ATP-dependent. At some time in the course of evolution, the bacterial Dha kinases must then have switched from ATP to the PTS as provider of high-energy phosphate. However, the core fold of DhaK could also point in an opposite direction. This structure appears in a number of PTS proteins, in the DhaM subunit of Dha kinases itself, in the IIA subunit of the mannose family of PTS transporters, and in the transcription regulator LevR of *Bacillus subtilis* (Fig. 5, black and gray). Whereas the amino acid sequence similarity between IIA^{Man}, DhaM, and LevR (Fig. 5, gray) is modest, it is nonexisting between the cores of DhaK and IIA^{Man} (Fig. 5, black and gray). It is noteworthy that a histidine and an aspartic acid are invariant at the topological switch point of each fold (Fig. 3). However, they perform different functions. His-66 and Asp-119 of DhaK bind the substrate by hydrogen bonding (Fig. 1*A*). His-10 of IIA^{Man} (His-9 of DhaM and His-585 of LevR) is phosphorylated, and Asp 67 of IIA^{Man} stabilizes and/or activates His-10 by formation of a hydrogen bond to the Nδ1 of the imidazole ring (9, 36).

DhaK of *E. coli* is the first, to our knowledge, and so far the only soluble carbohydrate phosphotransferase that utilizes the PTS as source of high-energy phosphate, all others being membrane proteins. It appears unlikely to us that DhaK could serve as a model for understanding the mechanism of vectorial phosphorylation by the carbohydrate transporters of the PTS (enzymes II). First, DhaK does not share amino acid sequence similarity with membrane-spanning domains of any PTS transporter, and second, phosphoryl groups are transferred directly from the IIA domain and not via a IIB domain as in transporters. In conclusion, DhaK is an example of a PTS protein, which is shared between bacteria and eukaryotes. Whether the common ancestor was a PTS protein or a kinase cannot yet be decided.

This work was supported by the Swiss National Science Foundation Grant 3100-063420 and the Ciba-Geigy Jubiläumsstiftung. Ta_6Br_{14} compound was a generous gift from Prof. Robert Huber, Max Planck Institute, Martinsried, Germany.

1. Luers, G. H., Advani, R., Wenzel, T. & Subramani, S. (1998) *Yeast* **14,** 759–771.
2. Nonomura, A. M. & Benson, A. A. (1992) *Proc. Natl. Acad. Sci. USA* **89,** 9794–9798.
3. Schurmann, M. & Sprenger, G. A. (2001) *J. Biol. Chem.* **276,** 11055–11061.
4. Fesq, H., Brockow, K., Strom, K., Mempel, M., Ring, J. & Abeck, D. (2001) *Dermatology (Basel)* **203,** 241–243.
5. Ivy, J. L. (1998) *Med. Sci. Sports Exercise* **30,** 837–843.
6. Taguchi, T., Murase, S. & Miwa, I. (2002) *Cell Biochem. Funct.* **20,** 223–226.
7. Beutler, R., Kämpfer, U., Schaller, J. & Erni, B. (2001) *Microbiology* **147,** 249–250.
8. Daniel, R., Stuertz, K. & Gottschalk, G. (1995) *J. Bacteriol.* **177,** 4392–4401.
9. Nunn, R. S., Markovic-Housley, Z., Génovésio-Taverne, J. C., Flükiger, K., Rizkallah, P. J., Jansonius, J. N., Schirmer, T. & Erni, B. (1996) *J. Mol. Biol.* **259,** 502–511.
10. Jia, Z., Vandonselaar, M., Hengstenberg, W., Quail, J. W. & Delbaere, L. T. (1994) *J. Mol. Biol.* **236,** 1341–1355.
11. Liao, D. I., Silverton, E., Seok, Y. J., Lee, B. R., Peterkofsky, A. & Davies, D. R. (1996) *Structure (London)* **4,** 861–872.
12. Gutknecht, R., Beutler, R., Garcia-Alles, L. F., Baumann, U. & Erni, B. (2001) *EMBO J.* **20,** 2480–2486.
13. Otwinowski, Z. & Minor, W. (1997) *Methods Enzymol.* **276,** 307–326.
14. Sheldrick, G. M. (1997) *Methods Enzymol.* **276,** 628–641.
15. de La Fortelle, E. & Bricogne, G. (1997) *Methods Enzymol.* **276,** 472–494.
16. Abrahams, J. P. & Leslie, A. W. G. (1996) *Acta Crystallogr. D* **52,** 30–42.
17. Perrakis, A., Morris, R. & Lamzin, V. S. (1999) *Nat. Struct. Biol.* **6,** 458–463.
18. Jones, T. A., Zou, J. Y. & Cowan, S. W. (1991) *Acta Crystallogr. A* **47,** 110–119.
19. Murshudov, G. N., Vagin, A. A., Lebedev, A., Wilson, K. S. & Dodson, E. J. (1999) *Acta Crystallogr. D* **55,** 247–255.
20. Holm, L. & Sander, C. (1991) *J. Mol. Biol.* **218,** 183–194.
21. Lowe, J. & Amos, L. A. (1998) *Nature* **391,** 203–206.
22. Cochran, A. G., Skelton, N. J. & Starovasnik, M. A. (2001) *Proc. Natl. Acad. Sci. USA* **98,** 5578–5583.
23. Richardson, J. S. & Richardson, D. C. (2002) *Proc. Natl. Acad. Sci. USA* **99,** 2754–2759.
24. Altschul, S. F., Gish, W., Miller, W., Myers, E. W. & Lipman, D. J. (1990) *J. Mol. Biol.* **215,** 403–410.
25. Wohrl, B. M., Wehmeier, U. F. & Lengeler, J. W. (1990) *Mol. Gen. Genet.* **224,** 193–200.
26. Orth, P., Schnappinger, D., Hillen, W., Saenger, W. & Hinrichs, W. (2000) *Nat. Struct. Biol.* **7,** 215–219.
27. Schumacher, M. A., Miller, M. C., Grkovic, S., Brown, M. H., Skurray, R. A. & Brennan, R. G. (2001) *Science* **294,** 2158–2163.
28. Allard, J., Grochulski, P. & Sygusch, J. (2001) *Proc. Natl. Acad. Sci. USA* **98,** 3679–3684.
29. Herz, S., Kis, K., Bacher, A. & Rohdich, F. (2002) *Phytochemistry* **60,** 3–11.
30. Fersht, A. (1999) in *Structure and Mechanism in Protein Science: A Guide to Enzyme Catalysis and Protein Folding* (Freeman, New York), p. 366.
31. Tessier, F. J., Monnier, V. M., Sayre, L. A. & Kornfield, J. A. (2002) *Biochem. J.* **369,** 705–719.
32. Molin, M., Norbeck, J. & Blomberg, A. (2003) *J. Biol. Chem.* **278,** 1415–1423.
33. Blomberg, A. (2000) *FEMS Microbiol. Lett.* **182,** 1–8.
34. Jin, R. Z., Forage, R. G. & Lin, E. C. (1982) *J. Bacteriol.* **152,** 1303–1307.
35. Johnson, E. A., Burke, S. K., Forage, R. G. & Lin, E. C. (1984) *J. Bacteriol.* **160,** 55–60.
36. Erni, B., Zanolari, B., Graff, P. & Kocher, H. P. (1989) *J. Biol. Chem.* **264,** 18733–18741.
37. Finan, T. M., Weidner, S., Wong, K., Buhrmester, J., Chain, P., Vorholter, F. J., Hernandez-Lucas, I., Becker, A., Cowie, A., Gouzy, J., *et al.* (2001) *Proc. Natl. Acad. Sci. USA* **98,** 9889–9894.
38. Bolotin, A., Wincker, P., Mauger, S., Jaillon, O., Malarme, K., Weissenbach, J., Ehrlich, S. D. & Sorokin, A. (2001) *Genome Res.* **11,** 731–753.